INFECTION AND IMMUNITY, Jan. 2005, p. 235–244 Vol. 73, No. 1
0019-9567/05/$08.00+0 doi:10.1128/IAI.73.1.235–244.2005

Fungal Metabolite Gliotoxin Targets Flavocytochrome b_{558} in the Activation of the Human Neutrophil NADPH Oxidase

Satoshi Nishida,[1,2] Lucia S. Yoshida,[1] Takashi Shimoyama,[1] Hiroyuki Nunoi,[3] Toshihiro Kobayashi,[4] and Shohko Tsunawaki[1]*

Department of Infectious Diseases, National Research Institute for Child Health and Development, Setagaya, Tokyo,[1] Department of Pediatrics, Miyazaki Medical College, University of Miyazaki, Kiyotake, Miyazaki,[3] Department of Anatomy and Cell Biology, Kochi Medical School, Kochi University, Nankoku, Kochi,[4] and Japan Science and Technology Corp., Kawaguchi, Saitama,[2] Japan

Received 6 July 2004/Returned for modification 13 August 2004/Accepted 15 September 2004

Fungal gliotoxin (GT) is a potent inhibitor of the O_2^--generating NADPH oxidase of neutrophils. We reported that GT-treated neutrophils fail to phosphorylate $p47^{phox}$, a step essential for the enzyme activation, because GT prevents the colocalization of protein kinase C βII with $p47^{phox}$ on the membrane. However, it remains unanswered whether GT directly affects any of NADPH oxidase components. Here, we examine the effect of GT on the NADPH oxidase components in the cell-free activation assay. The O_2^--generating ability of membranes obtained from GT-treated neutrophils is 40.0 and 30.6% lower, respectively, than the untreated counterparts when assayed with two distinct electron acceptors, suggesting that flavocytochrome b_{558} is affected in cells by GT. In contrast, the corresponding cytosol remains competent for activation. Next, GT addition in vitro to the assay consisting of flavocytochrome b_{558} and cytosolic components (native cytosol or recombinant $p67^{phox}$, $p47^{phox}$, and Rac2) causes a striking inhibition (50% inhibitory concentration = 3.3 μM) when done prior to the stimulation with myristic acid. NADPH consumption is also prevented by GT, but the in vitro assembly of $p67^{phox}$, $p47^{phox}$, and Rac2 with flavocytochrome b_{558} is normal. Posterior addition of GT to the activated enzyme is ineffective. The separate treatment of membranes with GT also causes a marked loss of flavocytochrome b_{558}'s ability to reconstitute O_2^- generation, supporting the conclusion at the cellular level. The flavocytochrome b_{558} heme spectrum of the GT-treated membranes stays, however, unchanged, showing that hemes remain intact. These results suggest that GT directly harms site(s) crucial for electron transport in flavocytochrome b_{558}, which is accessible only before oxidase activation.

Host defense against *Aspergillus* spp. depends mainly on the oxidative killing by superoxide anion (O_2^-)-derived reactive oxygen species (ROS) of neutrophils, as demonstrated by severe aspergillosis in patients with chronic granulomatous disease (9, 27, 51). The enzyme responsible for O_2^- generation is the multicomponent NADPH oxidase comprised of the membrane-integrated flavocytochrome b_{558} (a heterodimer of $gp91^{phox}$ and $p22^{phox}$) and four cytosolic regulatory proteins: $p67^{phox}$, $p47^{phox}$, $p40^{phox}$, and the small G-protein Rac2 (for reviews, see references 3, 14, 29, and 59). The N-terminal half of $gp91^{phox}$ contains four histidines coordinating two hemes according to a *bis*-heme motif (His101 and His209; His115 and His222) (5, 20), which is conserved in all members of the Nox (for NADPH oxidase)/Duox (for dual oxidase) family (for reviews, see references 35, 36, and 59). The C-terminal half of $gp91^{phox}$ has a reductase domain with binding sites for NADPH and FAD, which are also shared within the Nox/Duox members (for reviews, see references 35, 36, and 59).

In unstimulated neutrophils, the NADPH oxidase is kept dormant through maintaining its membrane and cytosolic components in the respective cellular locations under inactive conformation. However, upon cell stimulation with microbes or chemical agents, cytosolic components assemble with flavocytochrome b_{558} through a concerted series of molecular interactions among *Src* homology 3 (SH3) domains, proline-rich regions (PRR), *phox* homology (PX) domains, tetratricopeptide repeat (TPR) motifs, and other specific domains in $p47^{phox}$, $p67^{phox}$, $p22^{phox}$, and Rac2 (see reviews in references 3, 14, and 59). The steps involved in the assembly of an active NADPH oxidase complex have been elucidated as follows. (i) Phosphorylation of multiple serines in $p47^{phox}$ (19) opens its autoinhibited conformation kept by an intramolecular interaction between its SH3 domains and autoinhibitory region (AIR) (1, 25). (ii) The unmasked SH3 domains of $p47^{phox}$ then become able to target the PRR of $p22^{phox}$ (23, 39, 53), a key step in anchoring of the $p47^{phox}$-$p67^{phox}$-$p40^{phox}$ triad to flavocytochrome b_{558}. (iii) Rac2 translocates to the membrane, independently of the cytosolic *phox* components (15, 24), where it binds to the TPR motifs of $p67^{phox}$ (13, 30, 46) and with sites of flavocytochrome b_{558} not yet completely identified (12, 46) to cause conformational changes in flavocytochrome b_{558}. These interactions activate the $gp91^{phox}$ subunit of flavocytochrome b_{558} to flow electrons from NADPH to oxygen, in a sequence of events that involve its FAD and heme redox centers (59).

Although knowledge concerning the mechanism of the NADPH oxidase assembly has extensively been accumulated, not much is understood about how microbial pathogens escape the ROS-based defense in hosts. We have been investigating the effect of the fungal toxin, gliotoxin (GT), on the respiratory burst of human neutrophils (57, 62). GT is a natural and

* Corresponding author. Mailing address: Department of Infectious Diseases, National Research Institute for Child Health and Development, 2-10-1 Okura, Setagaya, Tokyo 157-8535, Japan. Phone: 81-3-3416-0181, x4820. Fax: 81-3-3417-2864. E-mail: tsunawaki@nch.go.jp.

biologically active metabolite of pathogenic fungi (60), such as *Aspergillus* and *Candida* spp., and is etiologically implicated in the establishment of severe infections in both animals (4) and humans (50). We have previously shown that GT inhibits the O_2^- generation of intact neutrophils before but not after the oxidase activation (62). The critical step affected by GT was the translocation of the cytosolic *phox* components to the membrane, which is triggered by the inhibited phosphorylation of $p47^{phox}$. The diminished $p47^{phox}$ phosphorylation was in good correlation with the decreased level of membrane-translocated protein kinase C βII (PKC βII) (57), the main kinase phosphorylating $p47^{phox}$ upon stimulation of neutrophils with phorbol myristate acetate (PMA) (10, 31). This event was a key mechanism underlying the prevented O_2^- generation in GT-treated intact cells. The inhibition of the NADPH oxidase by GT may play a critical role in the pathogenesis of *Aspergillus*-caused diseases such as aspergilloma and invasive aspergillosis, which involve mycelial growth in the body of the host. Since GT is produced during mycelial growth of pathogenic *Aspergillus* (60), the toxin would guarantee fungal survival through inhibiting the ROS-based killing of hyphae by neutrophils.

It is, however, still unanswered whether or not the above mechanism involving PKC βII (57) is the sole one responsible for the prevention of the oxidase activity. GT, a thiol-modifying toxin with an epipolythiodioxopiperazine structure (60), is expected to oxidize thiol groups of the NADPH oxidase components and directly compromise them. In the present study, we investigate this possibility by using the cell-free activation assay. This assay mimics the activation of the NADPH oxidase in vitro by incubating separated flavocytochrome b_{558} and cytosolic components in the presence of anionic amphiphiles as stimulants (6). We show that GT directly inhibits the electron transport of flavocytochrome b_{558}, only before but not after the oxidase activation.

MATERIALS AND METHODS

Materials. Antisera to the C-terminal polypeptides of $p67^{phox}$, $p47^{phox}$, and $p22^{phox}$ were raised in rabbits, as previously described (55, 56). Rabbit anti-Rac2 serum was purchased from Santa Cruz Biotechnology, Inc. (Santa Cruz, Calif.). Horseradish peroxidase-conjugated swine anti-rabbit immunoglobulin G and rabbit anti-goat immunoglobulin G were obtained from Dakopatts (Glostrup, Denmark). 4-Amidinophenylmethanesulfonyl fluoride (APMSF), cytochrome *c* (horse heart, type VI), *o*-dianisidine, diisopropyl fluorophosphate (DFP), dimethyl sulfoxide (DMSO), dithiothreitol (DTT), EDTA, EGTA, GT, guanosine 5′-[γ-thio]-triphosphate (GTPγS), *p*-iodonitrotetrazolium violet (INT), myristic acid (MA; sodium salt), protease inhibitors, and superoxide dismutase (SOD) were purchased from Sigma (St. Louis, Mo.); HEPES, PIPES [piperazine-*N*,*N*′-bis(2-ethanesulfonic acid)], and *n*-heptyl-β-D-thioglucoside (HTG) were from Dojindo Laboratories (Kumamoto, Japan); IPTG (isopropyl-β-D-thiogalactopyranoside), lysozyme from chicken egg white, NADPH, phenylmethylsulfonyl fluoride (PMSF), and sodium dodecyl sulfate (SDS) were from Wako Pure Chemical Industries (Tokyo, Japan). A protein assay and Macro-Prep ceramic hydroxyapatite type I (20 μm) were obtained from Bio-Rad Laboratories (Hercules, Calif.), and polyvinylidene difluoride sheets were from Millipore Corp. (Bedford, Mass.). Molecular markers for SDS-polyacrylamide gel electrophoresis (PAGE), protein A–Sepharose CL-4B, DEAE–Sepharose CL-6B, S Sepharose FF, and glutathione-Sepharose 4B were from Amersham Biosciences Corp. (Piscataway, N.J.). All other reagents used were of the highest grades available.

Subcellular fractionation of neutrophils. Human fresh blood or buffy coat residues were obtained in accordance with the protocol approved by our Institutional Review Board for Human Subjects, and neutrophils were isolated as reported previously (55). The isolated neutrophils were then treated with 2 mM DFP for 15 min on ice before fractionation into membranes and cytosol in buffer A (100 mM KCl, 3 mM NaCl, 3.5 mM $MgCl_2$, and 10 mM PIPES [pH 7.3]) containing 10 μM leupeptin and 1 mM PMSF, essentially as previously described (56). In some cases, the membranes were further washed with 1 M NaCl in buffer A for 10 min and solubilized at 5 mg of protein/ml by stirring for 30 min on ice in 50 mM sodium phosphate buffer (pH 7.0) containing 50 mM NaCl, 1% (wt/vol) HTG, 25% (wt/vol) glycerol, and 1 mM APMSF (42). HTG-solubilized membranes were then recovered by centrifugation at 100,000 × *g* for 30 min at 4°C. When mentioned, the neutrophils were incubated as previously described (57) with 10 μg (30.6 nmol) of GT/0.25 × 10^7 cells/ml for 10 min at 37°C, a condition shown to completely inhibit their NADPH oxidase activity in response to PMA stimulation (57), before being washed and fractionated into membranes and cytosol. Matched control neutrophils were similarly treated with DMSO vehicle instead of GT and then fractionated. These fractions were tested for O_2^--reconstituting ability in the cell-free activation assay as described below. Protein concentration was determined by the method of Lowry using bovine serum albumin as a standard. Flavocytochrome b_{558} content in the membrane fraction was expressed in heme equivalents determined by a reduced-minus-oxidized difference spectrum analysis as described below.

Preparation of recombinant cytosolic components. The insect *Spodoptera frugiperda* Sf9 cells were cultured in Grace's medium (Life Technologies, Grand Island, N.Y.) containing 10% (vol/vol) fetal calf serum (JHR Biosciences, Lenexa, Australia), as well as 0.3% (wt/vol) lactoalbumin hydrolysate and 0.3% (wt/vol) yeastolate (both from Life Technologies). Baculoviruses containing cDNAs for human $p47^{phox}$ and $p67^{phox}$ (58) were generous gifts from J. D. Lambeth (Emory University, Atlanta, Ga.). Monolayer cultures of the Sf9 cells were infected with the recombinant baculoviruses in 100-mm-diameter dishes, harvested 84 h after the infection, and then frozen in liquid nitrogen. Recombinant proteins (*r*$p47^{phox}$ and *r*$p67^{phox}$) were purified essentially based on reported methods (38). Briefly, the Sf9 cells were resuspended in buffer A containing 0.1 mM APMSF, 2 mM DFP, and 0.1 mM DTT; disrupted by sonication with 12 10-s pulses at 200 W (Sonifier 450 apparatus; Branson Ultrasonic Corp., Danbury, Conn.); and centrifuged at 12,000 × *g* for 10 min at 4°C. The supernatant was subsequently centrifuged at 100,000 × *g* for 1 h at 4°C to obtain crude extract. The crude extract containing *r*$p47^{phox}$ was applied to an S Sepharose FF column equilibrated with 5 mM potassium phosphate buffer (pH 7.0) and eluted with a gradient of 0 to 0.3 M NaCl in the same buffer. The crude extract containing *r*$p67^{phox}$ was applied to a DEAE–Sepharose CL-6B column equilibrated with 20 mM Tris-HCl (pH 7.5) and eluted with a gradient of 0 to 0.5 M NaCl in the same buffer. Peak fractions of *r*$p67^{phox}$ were pooled and further loaded onto a ceramic hydroxyapatite type I column equilibrated with 10 mM potassium phosphate buffer (pH 7.0) and eluted with a gradient of 0.01 to 0.6 M potassium phosphate buffer (pH 7.0). Throughout all of the column work, the buffers were supplemented with 0.1 mM DTT and 0.15 mM APMSF. The purity of the recombinant proteins was assessed by SDS-PAGE plus subsequent Coomassie blue staining; 99% (*r*$p47^{phox}$) and 90% (*r*$p67^{phox}$) purity were confirmed (Fig. 2A, inset), respectively, by the analysis with a pdi 420oe scanner (Arcus II; PDI, Inc., Huntington Station, N.Y.).

Recombinant Rac2 was isolated from XL1-Blue MRF′ *Escherichia coli* transformed with human Rac2 cDNA subcloned into the bacterial expression vector, pGEX2T, as previously described (34). The transformed *E. coli* cells were grown at 20°C in Luria-Bertani medium containing 100 μg of ampicillin/ml to an A_{600} of 0.6 and induced with 0.1 mM IPTG for 6 h before harvest by centrifugation. The pelleted bacteria were resuspended in 25 mM HEPES buffer (pH 7.6) with 1 mM EDTA and then frozen in liquid nitrogen before storage at −80°C. The frozen cell suspension was thawed on ice and adjusted to 80 mM KCl, 2 mM DTT, and 0.3 mg of lysozyme/ml. After a 20-min standing on ice, the freezing and thawing was repeated once again to obtain cell lysate. The cell lysate was clarified by centrifugation at 100,000 × *g* for 20 min at 4°C and applied onto a glutathione-Sepharose 4B column. Rac2 was then cleaved from the fusion protein on the resin by thrombin treatment. The purity of Rac2 was 80%. The concentration of the recombinant proteins was determined by the method of Bradford with bovine serum albumin as a standard.

Cell-free activation of the NADPH oxidase. The amphiphile-stimulated activation of the NADPH oxidase in the cell-free assay was done with various combinations of flavocytochrome b_{558} (in membranes before or after HTG solubilization) and cytosolic components (native cytosol or recombinant proteins), as detailed in the legends. MA was used as a stimulant at optimal amounts for best activation in each assay system. Furthermore, a two-step activation protocol was adopted: the components were first preincubated for 5 min at room temperature in plastic cuvettes with or without MA in volumes of 0.1 to 0.4 ml of activation buffer (65 mM sodium phosphate buffer [pH 7.0] containing 1.2 mM $MgCl_2$, 1 mM EGTA, and 2 mM NaN_3) and then brought to 0.8 ml with the activation buffer containing an appropriate electron acceptor. The stimulation with MA was performed in the presence of 5 μM GTPγS for native cytosol. For

the semirecombinant cell-free assay, purified Rac2 was incubated with a fivefold molar excess of GTPγS for 5 min at room temperature before use (32). Three distinct electron acceptors (30 μM cytochrome *c*, 30 μM acetylated cytochrome *c*, and 50 μM INT) were used becuase of their properties as electron flow indicators. The reaction was usually started by adding 0.2 mM NADPH to the mixture in a Hitachi 557 spectrophotometer. For assays with native and acetylated cytochrome *c* as indicators, 200 U of SOD/ml was added at maximum velocities to distinguish the reduction by O_2^- from nonspecific reduction. The acetylated cytochrome *c* was prepared as previously reported (54). The efficiency of the acetylated compound in detecting O_2^- from PMA-stimulated neutrophils was 36.4% of that of native cytochrome *c*, which was taken into account in the calculation. The molar extinction coefficients for calculation were $\varepsilon_{550\text{-}540\ nm}$ = 19.1 $mM^{-1}\ cm^{-1}$ for native and acetylated cytochrome *c* and $\varepsilon_{500\ nm}$ = 11 $mM^{-1}\ cm^{-1}$ for INT, respectively. The consumption of NADPH (0.125 mM) was quantified by the rate of absorbance decrease at 340 nm.

Cell-free assembly of flavocytochrome b_{558} with cytosolic components. The ability of flavocytochrome b_{558} to assemble with cytosolic *phox* components upon cell-free activation was evaluated by immunoprecipitation with anti-p47^{phox} serum, as follows. HTG-solubilized membranes (2.5 pmol of heme equivalent of flavocytochrome b_{558}), 8.5 pmol of *r*p47^{phox}, and 3 pmol of *r*p67^{phox} were incubated with either 30 nmol of GT or DMSO vehicle for 5 min at room temperature in 0.2 ml of activation buffer. The treated components were then stimulated with 27.5 nmol of MA for 10 min prior to immunoreaction with the anti-p47^{phox} serum or normal serum for 90 min on ice in 0.8 ml of immunoprecipitation buffer (150 mM NaCl, 10 mM EDTA, 1% [wt/vol] deoxycholate, and 1% [wt/vol] Nonidet P-40 in 10 mM Tris-HCl [pH 7.4]). P47^{phox} was then precipitated with 4 mg of protein A–Sepharose CL-4B, as previously reported (56). The translocation of Rac2 to flavocytochrome b_{558} was assessed by analysis of the activated oxidase complex after centrifugation on a sucrose gradient, as previously described (56). Briefly, the reaction mixture consisting of unsolubilized membranes (6 pmol of heme equivalent), 252 pmol of *r*p47^{phox}, 36 pmol of *r*p67^{phox}, and 252 pmol of GTPγS-loaded Rac2 in 0.4 ml of activation buffer was treated with either 60 nmol of GT or DMSO vehicle for 5 min at room temperature. After stimulation with 80 nmol of SDS for 5 min, the reaction mixture was layered onto a discontinuous sucrose gradient composed of 0.85 ml of 15% (wt/vol) over 0.05 ml of 50% (wt/vol) in the activation buffer and centrifuged at 109,000 × *g* for 30 min at 4°C. The membranes were recovered from the 50% sucrose bottom and washed once with the activation buffer at 4°C. The above-described immunoprecipitates and the washed membranes were resuspended in 5% SDS sample buffer containing 100 mM DTT and then boiled for 5 min at 100°C before SDS-PAGE (10% gel). The presence of flavocytochrome b_{558}, p47^{phox}, and p67^{phox} was confirmed by immunoblotting with antisera to p22^{phox}, p47^{phox}, and p67^{phox}, respectively, followed by probing with horseradish peroxidase-conjugated secondary serum plus *o*-dianisidine development. The presence of Rac2 was checked with anti-recombinant Rac2 serum and visualized with Enhanced Chemiluminescence(ECL)-Plus reagents (Amersham).

Reduced-minus-oxidized difference spectrum of flavocytochrome b_{558}. Membranes containing 75 pmol of heme equivalent of flavocytochrome b_{558} were incubated with 153 nmol of GT for 15 min at room temperature in buffer A, recovered by centrifugation at 100,000 × *g* at 4°C, and washed with the same buffer. The GT-treated membranes were then resuspended and subjected to the spectrum analysis of flavocytochrome b_{558} with a Hitachi 557 spectrophotometer after sample bubbling with standard CO gas (99.9% pure; Nippon Sanso, Tokyo, Japan) in a black quartz cuvette, as previously reported (61). Reduced-minus-oxidized spectra were recorded at different times after the addition of a few crystals of sodium dithionite. Molar extinction coefficients of $\varepsilon_{558\text{-}540\ nm}$ = 21.6 $mM^{-1}\ cm^{-1}$ (7) and $\varepsilon_{426\text{-}410\ nm}$ = 200 $mM^{-1}\ cm^{-1}$ (41) were used to calculate the alpha and Soret peaks, respectively.

RESULTS

Which cellular target, membrane or cytosolic components, is affected by GT in intact neutrophils? The neutrophil NADPH oxidase is composed of the membrane-integrated flavocytochrome b_{558} and cytosolic components. We investigated here whether the treatment of intact neutrophils with GT directly compromises any of the NADPH oxidase components. For this purpose, the isolated membranes and cytosol from GT-treated neutrophils were tested for the ability to reconstitute O_2^- generation in the cell-free activation assay. In the assay, an anionic amphiphile such as MA or SDS is used as a stimulant (6, 44) to provoke the disruption of the autoinhibited state of p47^{phox}, necessary to allow its association with the p22^{phox} subunit of flavocytochrome b_{558}, as well as with p67^{phox}, eventually leading to oxidase activation (1, 21, 23, 25, 39, 53, 59). The cell-free activation assay thus allows the verification of the integrity of the oxidase components in reconstituting the enzyme activity.

The cellular target of GT was searched by cross-combination assays between membranes and cytosol obtained from GT-treated and untreated neutrophils. When both fractions were from untreated cells, a 10-min stimulation with MA allowed high O_2^- generation after the addition of NADPH, shown by a typical chart of SOD-sensitive cytochrome *c* reduction (65.3 mol of O_2^-/s/mol of heme) (Fig. 1Aa). Membranes from GT-treated cells combined with the cytosol from untreated cells also allowed the activation of the NADPH oxidase, but with a rate around 40% lower (37.3 mol of O_2^-/s/mol of heme) (Fig. 1Ab) than the combination of the untreated cell fractions. When both the fractions were from GT-treated cells, an unexpectedly high rate of cytochrome *c* reduction appeared even before the addition of NADPH, but it rapidly ceased without SOD (Fig. 1Ac). This apparent "direct reduction" (i.e., without mediation by O_2^-) made the assays with cytochrome *c* unsuitable for judging O_2^- generation.

The direct cytochrome *c* reduction was pertaining to the cytosol from the GT-treated cells, since the cytosol alone plus cytochrome *c* induced rapid reduction in the absence of membranes and MA (Fig. 1Ba). Neither NADPH nor SOD influenced the rate of cytochrome *c* reduction (Fig. 1Ca). In contrast, the cytosol from the untreated cells (Fig. 1Bb) and the membranes from GT-treated cells (Fig. 1Bc) both gave minimal rates. These results indicate that the direct cytochrome *c* reduction originates from a reaction between the cytosol and GT in cells. GT alone was ineffective in reducing cytochrome *c* (data not shown). Since this side reaction of GT was very unfavorable to determine net O_2^- generation, two other electron acceptors, INT and acetylated cytochrome *c*, were tested. INT was shown to receive electrons from hemes of flavocytochrome b_{558} (49), and acetylated cytochrome *c*, to be reduced by O_2^- with far less susceptibility to reduction by cellular cytochrome *c* reductases (43). INT was not susceptible to the direct reduction: the cytosol from the GT-treated cells gave flat kinetics with INT (Fig. 1Cc) in contrast to that with cytochrome *c* (Fig. 1Ca). Acetylated cytochrome *c* also yielded a significantly lower rate (Fig. 1Cb). These electron acceptors have clearly demonstrated that the direct cytochrome *c* reduction observed with the cytosol from the GT-treated cells is not assigned to the NADPH oxidase activity.

Finally, the cell-free combination assays with the membranes and cytosol from the GT-treated cells in Fig. 1A were remade by using the two electron acceptors. The oxidase activity determined in the assays with INT and acetylated cytochrome *c* is summarized in Table 1. Once intact neutrophils had been treated with GT, their subsequent membrane component functioned less efficiently in the cell-free activation assays: the membranes from the GT-treated cells showed 40.0 and 33.8% (INT) and 30.6 and 25.8% (acetylated cytochrome *c*) lower activities with the cytosol from the untreated and GT-treated cells, respectively. In contrast, the cytosol from the GT-treated

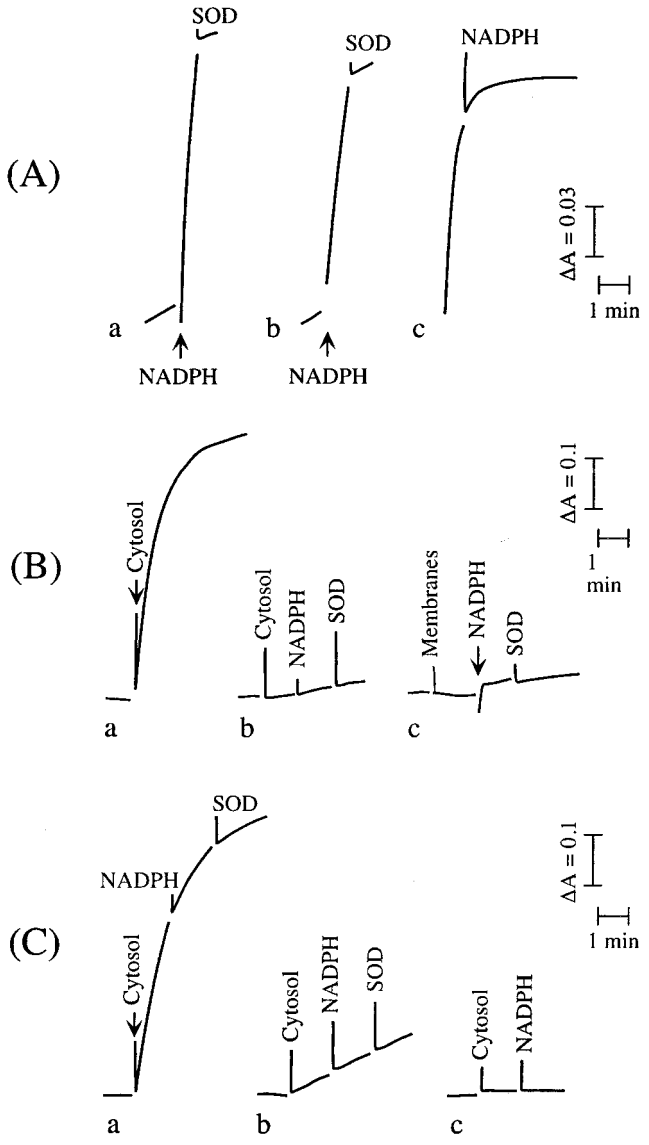

FIG. 1. Direct reduction of cytochrome *c* by the cytosol reacted with GT. Neutrophils were treated with GT (10 μg = 30.6 nmol of GT/0.25×10^7 cells/ml; +GT) or DMSO vehicle alone (−GT) for 10 min at 37°C, washed, and fractionated into membranes and cytosol, which were subsequently tested for their properties as below. (A) Cell-free activation. Mixtures containing membranes (15 μg of protein: 3 pmol of heme equivalent of flavocytochrome b_{558}) plus cytosol (250 μg) were stimulated with 80 nmol of MA for 10 min at room temperature. Charts show a combination of the fractions from cells (−GT) (a), membranes from cells (+GT) plus cytosol from cells (−GT) (b), and both from cells (+GT) (c). Note that in chart c, a striking direct cytochrome *c* reduction occurs before NADPH addition. (B) Verification of the origin of the direct cytochrome *c* reduction. Cytosol (50 μg) and membranes (1.5 pmol of heme equivalent) were added to separate cuvettes containing cytochrome *c*, and its reduction was recorded in the absence of MA. Charts show cytosol [(+GT) (a), cytosol (−GT) (b), and membranes (+GT)] (c). (C) Assays with INT and acetylated cytochrome *c*. The cytosol from cells (+GT) was added to a cuvette containing cytochrome *c* (a), acetylated cytochrome *c* (b), or INT (c) as an electron acceptor. Reactions were started by the addition of cytosol (+GT). Where indicated, 0.2 mM NADPH and 200 U of SOD/ml were added to the cuvettes. The charts are representative of two experiments done in duplicate.

TABLE 1. Cell-free combination assay with membranes and cytosol from GT-treated and untreated neutrophils

Medium	Mean NADPH oxidase activity[a] (%) ± SD			
	INT with membranes		Acetylated cytochrome *c* with membranes	
	−GT	+GT	−GT	+GT
Cytosol without GT	100.0 ± 7.8	60.0 ± 1.6*	100.0 ± 6.4	69.4 ± 4.6*
Cytosol with GT	94.6 ± 5.2	66.2 ± 10.3†	106.6 ± 10.0	74.2 ± 3.0†

[a] Membranes (15 μg of protein: 3 pmol of heme equivalent) and cytosol (250 μg) isolated from neutrophils treated with (+) or without (−) GT (10 μg = 30.6 nmol of GT/0.25×10^7 cells/ml for 10 min at 37°C) were cross-combined for the stimulation with 80 nmol of MA (see Materials and Methods). After a 5-min incubation, kinetics were started by the addition of 0.2 mM NADPH to the cuvette. Rates are expressed as the percentage of the control assays with fractions from GT-untreated neutrophils (100%; 13.8 ± 1.1 mol of INT/s/mol of heme by the INT assay and 37.9 ± 2.4 mol of O_2^-/s/mol of heme by the acetylated cytochrome *c* assay, respectively). Data show the means of two experiments done in duplicate. * and †, Significantly different from the corresponding activity with the fractions from GT-untreated neutrophils at both $P < 0.04$ and $P < 0.1$, respectively, as determined by the Student *t* test (two-tailed test for independent samples).

cells kept full competence to support the cell-free activation when combined with the membranes from the untreated cells. The results of the combination experiments suggest that GT directly affects a component of the NADPH oxidase at the cellular level, probably the membrane component flavocytochrome b_{558}.

Direct effect of GT on the NADPH oxidase during cell-free activation. We next investigated whether GT is able to exert direct effect(s) on NADPH oxidase components when included during enzyme activation in the cell-free assay. In preliminary experiments we had noted that the above GT-induced direct cytochrome *c* reduction occurs even in the assay with the membrane and cytosol from untreated cells (data not shown), maybe because the presence of GT during preincubation with native cytosol causes such an effect. Thus, we here substituted the cytosol with recombinant cytosolic components *r*p67^{phox}, *r*p47^{phox}, and Rac2 (Fig. 2A, inset) and reconstituted O_2^- generation, together with membranes in the presence of MA. The use of the recombinant proteins succeeded to obviate the direct cytochrome *c* reduction, as demonstrated by the null background rate in the assay (Fig. 2A, +GT). This result confirms that the direct cytochrome *c* reduction in Fig. 1 originated from reactions between GT present in the cytosol of GT-treated cells and reactants other than the NADPH oxidase components. This semirecombinant assay has clearly demonstrated that GT is able to directly inhibit the NADPH oxidase activation (95% inhibition with 100 nmol of GT) (Fig. 2A, +GT versus −GT). The 50% inhibitory concentration (IC_{50}) of GT preadded into the semirecombinant assay with 1 pmol of heme equivalent of flavocytochrome b_{558} was 3.3 μM (1.1 μg/ml) (Fig. 2B). The IC_{50} of GT preadded into the assay mixture consisting of HTG-solubilized flavocytochrome b_{558} plus native cytosol (1.5 pmol of heme equivalent plus 100 μg of cytosol; evaluated with acetylated cytochrome *c*) was exactly the same as in the semirecombinant assay (data not shown).

The order of GT addition to the semirecombinant assay, whether before or after the stimulation with MA, made a striking difference in the degree of enzyme inhibition: a marked drop of oxidase activity was observed for a prior addition (Fig. 3, closed bars). In contrast, a posterior addition of GT showed

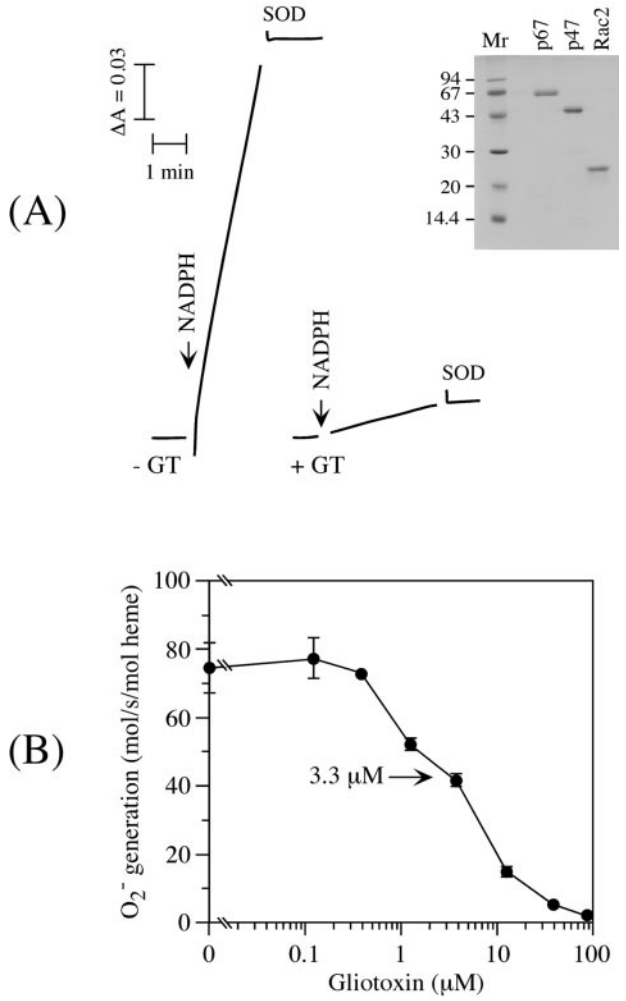

FIG. 2. Effect of GT on the cell-free activation of NADPH oxidase. The effect of GT on the reconstitution of NADPH oxidase was examined by semirecombinant cell-free system. (A) The reaction mixture consisting of HTG-solubilized membranes (1 pmol of heme equivalent of flavocytochrome b_{558}) plus recombinant cytosolic components (36 pmol of *r*p67^{phox}, 252 pmol of *r*p47^{phox}, and 252 pmol of GTPγS-loaded Rac2) was incubated with 30 nmol of GT (+GT) or DMSO vehicle (−GT) for 3 min at room temperature and then stimulated with 27.5 nmol of MA for an additional 5 min in 0.2 ml of activation buffer. After dilution to 0.8 ml, O_2^- generation was evaluated by the reduction of cytochrome *c*. Note the absence of the SOD-insensitive direct reduction of cytochrome *c* contrasting with the assay where native cytosol was used (Fig. 1A). The charts are representative of six experiments done in duplicate. The purity of the cytosolic components is shown in the inset. (B) GT dose-dependent inhibition of the NADPH oxidase activity in the semirecombinant assay shown in panel A, except that GT was added 5 min before the MA stimulation. The arrow indicates an IC_{50} of 3.3 μM. GT concentrations are relative to the final volume of 0.8 ml. The data represent the means ± the standard deviations of two experiments done in duplicate.

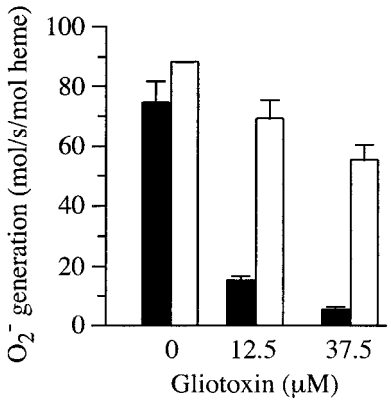

FIG. 3. Postaddition effect of GT on the cell-free activation of NADPH oxidase. The NADPH oxidase activation was performed as in Fig. 2A by using a semirecombinant cell-free assay. For preaddition (■) and postaddition (□) effects, GT was added 3 min before and after a 5-min stimulation with MA, respectively. The data represent the means ± the standard deviations of two experiments done in duplicate.

a less pronounced inhibition (Fig. 3, open bars). The slight inhibition with the posterior addition of GT probably reflects that the activation process has not yet been completed in the 5-min stimulation period with MA. This conclusion is based on the previous observation (57) that the later addition of GT to membranes isolated from PMA-stimulated cells, in which the NADPH oxidase is already assembled, did not affect the enzyme activity at all. The same behavior of GT inhibition seen in Fig. 3 was observed in assays with native cytosol as well (data not shown). These results suggest that GT has no effects on the catalysis of the activated NADPH oxidase.

Next, the effect of GT on the consumption of the electron donor, NADPH, was examined for the NADPH oxidase reconstituted in vitro with membranes and cytosol from untreated neutrophils. When the NADPH oxidase was activated with MA, it consumed NADPH to generate O_2^- (Fig. 4a). In contrast, null NADPH consumption was observed for the unstimulated oxidase (Fig. 4b). GT present during the stimulation with MA prevented the NADPH consumption by the oxi-

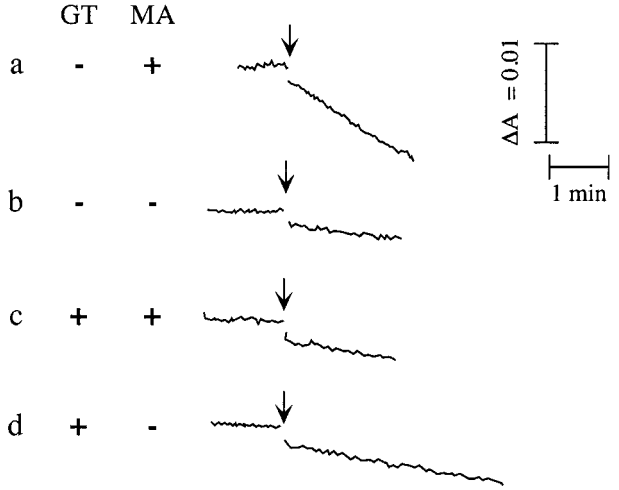

FIG. 4. Effect of GT on NADPH consumption. HTG-solubilized membranes (1.5 pmol of heme equivalent) and cytosol (100 μg) were incubated in the absence (a and b) or presence (c and d) of 92 nmol of GT for 3 min in 0.1 ml of activation buffer (see Materials and Methods) before a 5-min stimulation with 36 nmol of MA. The mixture was then transferred at the point indicated by the arrow to a cuvette preset in the spectrophotometer containing NADPH (final concentration, 0.125 mM) in the activation buffer. A decrease in the absorbance at 340 nm indicates NADPH consumption.

TABLE 2. O_2^--generating ability of flavocytochrome b_{558} treated with GT in vitro

Medium conditions	NADPH oxidase activity[a]	
	Mean amt (mol/s/mol of heme) ± SD	Mean % inhibition ± SD
−GT	26.6 ± 0.3	0.0 ± 1.1
+GT	4.6 ± 0.6	82.7 ± 2.3

[a] Membranes from untreated neutrophils were treated in vitro with GT (2 nmol of GT/pmol of heme; see the legend for Fig. 6) and washed by centrifugation. One picomole of heme equivalent of flavocytochrome b_{558} was then combined with recombinant cytosolic components (252 pmol of *r*p47^{phox}, 36 pmol of *r*p67^{phox}, and 252 pmol of GTPγS-loaded Rac2) for the reconstitution of NADPH oxidase activity in a cell-free assay (see Materials and Methods). O_2^- generation was determined by the cytochrome *c* assay. Data show the means of two experiments done in duplicate.

dase (Fig. 4c). GT was previously suggested to consume NADPH for redox cycling reactions, which occur in the presence of oxygen between the disulfide and thiol forms of GT at the expense of cellular reductants such as NADPH (18, 45). However, the incubation of membranes and cytosol with GT in the absence of MA did not consume NADPH (Fig. 4d). Thus, the inhibition of cell-free activation with GT is unlikely to result from the depletion of the substrate, NADPH, by the redox cycling reactions.

The inhibition of O_2^- generation described above was completely canceled by the simultaneous addition of DTT with GT or when the *S*-methylated compound of GT, *bis*-dethio-*bis*-(methylthio)-GT, was used instead of GT (data not shown). The results show that the disulfide bridge of GT is crucial for its inhibitory effect on the cell-free activation of the oxidase, as it was in the case of intact cells (57). These findings have proved that GT directly inhibits the process of enzyme activation in the cell-free assay.

Effect of treatment of flavocytochrome b_{558} with GT on its cell-free reconstituting ability. Since the cell-free combination experiments in Table 1 suggested that GT is likely to affect the membrane component of the oxidase in intact cells, we here treated flavocytochrome b_{558} of isolated membranes in vitro with GT and tested for its subsequent activity in the cell-free activation assay. For this test, membranes (75 pmol of heme equivalent of flavocytochrome b_{558}) from untreated cells were treated with GT for 15 min and washed twice to remove unreacted GT. Their O_2^--generating activity was then evaluated after incubation with recombinant cytosolic components in the presence of MA (Table 2). The oxidase activity decreased by 82.7% of the DMSO vehicle control, showing a significant inactivation of the GT-treated flavocytochrome b_{558}. The inhibition by 82.7% also indicates that a large part of the inhibition seen in the aforementioned cell-free activation assays (Fig. 2) was assigned to the effect of GT on flavocytochrome b_{558} itself.

Two ways of affecting the functionality of flavocytochrome b_{558} are possible: (i) compromising the ability of flavocytochrome b_{558} to assemble with cytosolic components and (ii) altering the redox centers in the gp91^{phox} subunit needed for normal electron transport directly or indirectly through conformational change(s) that affect enzyme catalysis. These possibilities were examined and are discussed below.

Effect of GT on the ability of flavocytochrome b_{558} to assemble with cytosolic components. The assembly of the NADPH oxidase in vitro is triggered by the disruption of p47^{phox} intramolecular binding between its SH3 domains and the AIR with amphiphiles such as MA and SDS, which allows subsequent associations of the unmasked SH3 domains and its C-terminal PRR with the PRR of p22^{phox} and the C-terminal SH3 of p67^{phox}, respectively (1, 21, 23, 25, 39, 53, 59). Here, we tested flavocytochrome b_{558} for the ability to assemble with cytosolic components upon cell-free activation in the presence or absence of GT. The interaction of flavocytochrome b_{558} with *r*p47^{phox} and *r*p67^{phox} was verified first in the absence of Rac2 by immunoprecipitation with anti-p47^{phox} serum. As mentioned above, MA stimulation induces the association of p47^{phox} and p67^{phox} (which is recruited via p47^{phox}) with flavocytochrome b_{558}, and thus the three components are recovered in the immunoprecipitate with the anti-p47^{phox} serum (Fig. 5A, lane 1 versus lane 2; see the immunoblotted bands of p22^{phox}

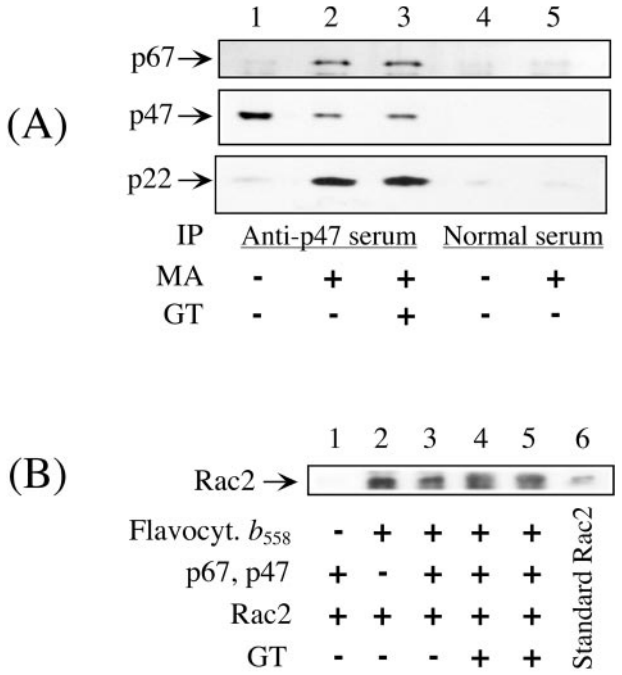

FIG. 5. Effect of GT on in vitro assembly of flavocytochrome b_{558} with cytosolic components. (A) Analysis of p67^{phox} and p47^{phox} association with flavocytochrome b_{558}. HTG-solubilized membranes (2.5 pmol of heme equivalent) were incubated with *r*p67^{phox} (3 pmol) and *r*p47^{phox} (8.5 pmol) in the presence (+) or absence (−) of 30 nmol of GT for 5 min and subsequently stimulated with 27.5 nmol of MA for 10 min at room temperature. The mixture was then subjected to immunoprecipitation (IP) with anti-p47^{phox} serum or normal serum and analyzed by immunoblotting plus development with *o*-dianisidine (see Materials and Methods). (B) Analysis of Rac2 membrane translocation. Membranes (6 pmol of heme equivalent) were combined with *r*p67^{phox} (36 pmol), *r*p47^{phox} (252 pmol), and GTPγS-loaded Rac2 (252 pmol) in 0.4 ml of activation buffer in the presence or absence of 60 nmol of GT for 5 min at room temperature. The mixture was then stimulated with 80 nmol of SDS for an additional 5 min, followed by loading onto a discontinuous sucrose gradient (15% over 50%) and centrifugation (see Materials and Methods). The membrane pellet containing assembled NADPH oxidase was recovered and analyzed by immunoblotting with anti-Rac2 serum, followed by detection with an ECL-Plus reaction. Lane 5 shows the addition of GT 5 min after the SDS stimulation, and lane 6 was loaded with 2 pmol of recombinant Rac2. The data are representative of two (A) or three (B) experiments.

and p67^{phox}). GT did not affect the interactions among the three, as shown by the unchanged recoveries of p22^{phox} and p67^{phox} in the immunoprecipitate (Fig. 5A, lane 3). This observation was also confirmed by the alternative immunoprecipitation with anti-p67^{phox} serum (data not shown). No bands appeared when normal serum was used for immunoprecipitation (Fig. 5A, lanes 4 and 5). Rac2 was omitted in the experiments because it is known to translocate to the membrane component independently of p47^{phox} and p67^{phox} (15, 24). Also, lower amounts of *r*p47^{phox} (8.5 pmol) and of *r*p67^{phox} (3 pmol), in a ratio reflecting their content in the neutrophil (28, 38), compared to those for the cell-free O_2^- generation (Fig. 2A), were used in the immunoprecipitation assay because the anti-*r*p47^{phox} serum also precipitates the majority of *r*p47^{phox} not associated with p22^{phox}.

The ability of flavocytochrome b_{558} to assemble with Rac2, including p47^{phox} and p67^{phox}, was evaluated by analysis of the components in the membrane fraction recovered by sucrose density-gradient centrifugation after SDS stimulation (Fig. 5B). Flavocytochrome b_{558} associated normally with p67^{phox} and p47^{phox} in the presence of GT (data not shown), confirming the results in Fig. 5A. The recruitment of Rac2 to the complex, which does not depend on the presence of p47^{phox} and p67^{phox} (Fig. 5B, lane 2) (17, 24), was unaffected by GT, regardless of its addition before or after oxidase activation with SDS (Fig. 5B, lanes 4 and 5). These results by the two different methods demonstrated that GT does not compromise the ability of flavocytochrome b_{558} to assemble with the cytosolic components.

Heme spectrum analysis of GT-treated flavocytochrome b_{558}. The effect of GT on the hemes of flavocytochrome b_{558} was analyzed by oxidized-minus-reduced difference spectra of membranes treated with GT for 15 min at room temperature. The spectrum showed the same features as those of GT-untreated control membranes, indicating that the hemes were kept intact (Fig. 6). Specifically, a decrease in heme content and shifts in characteristic peaks at 426 nm (Soret) and at 558 nm (alpha) could not be detected, showing that the hemes of the GT-treated flavocytochrome b_{558}, specifically in the gp91^{phox} subunit, were likely to maintain the normal coordination and shape.

Other possible target(s) of GT in gp91^{phox} could be the domains involved in the binding of NADPH and FAD, whose functions depend on appropriate conformational changes during the process of enzyme activation (59). The reduction of INT, an electron flow indicator of the NADPH oxidase (49), was also inhibited by GT in the cell-free activation assay (data not shown), in agreement with the inhibition at the cellular level (Table 1). Moreover, since NADPH consumption was also inhibited by GT (Fig. 4), it is most likely that GT disables the electron flow from NADPH to hemes by affecting site(s) required for the redox function of flavocytochrome b_{558} but not its assembly with the cytosolic components p67^{phox}, p47^{phox}, and Rac2.

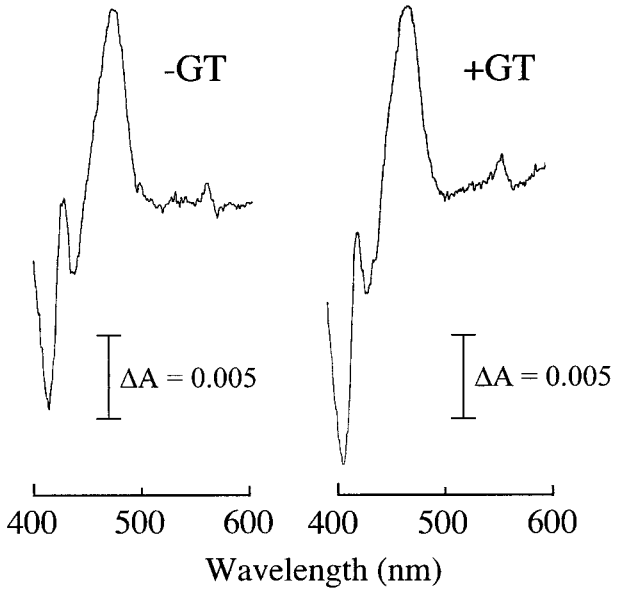

FIG. 6. Effect of GT on the difference spectrum of flavocytochrome b_{558}. Membranes (75 pmol of heme equivalent) were treated with 153 nmol of GT for 15 min at room temperature and washed by centrifugation before the determination of dithionite-reduced-minus-oxidized spectra of flavocytochrome b_{558} (see Materials and Methods). One-third aliquots were transferred to black cuvettes for the spectral analysis. Representative difference spectra at least 5 min after the dithionite addition to untreated (−GT) and GT-treated (+GT) membranes are shown. The amounts of heme calculated from the Soret peaks at 426 nm were ca. 23 pmol in both cases and fit well with the expected theoretical value of 25 pmol. The GT-treated membranes were unable to reconstitute O_2^- generation when combined with recombinant cytosolic components in the presence of MA (see Table 2). The data are representative of three experiments.

DISCUSSION

Considering the early known high sensitivity of NADPH oxidase toward thiol modifiers, such as *N*-ethylmaleimide (2, 47), *p*-chloromercuribenzoate (8, 22, 48), and phenylarsine oxide (PAO) (16, 33, 37, 40), the possibility of the fungal metabolite GT, having a disulfide bridge, to react with NADPH oxidase components was fairly conceivable. We have demonstrated at the cellular level that GT imposes damage to the respiratory burst of neutrophils by inhibiting protein kinase C βII-related responses: p47^{phox} phosphorylation, its incorporation to the cytoskeleton, and the subsequent membrane translocation of p67^{phox} and p47^{phox} (57). However, it remained unresolved whether GT can also directly affect the NADPH oxidase components. We show here that GT directly affects flavocytochrome b_{558} not only in intact cells but also in the cell-free activation assay.

In the present study, in order to specify the cellular target of GT in intact cells, whether membrane or cytosolic components, we adopted acetylated cytochrome *c* and INT as electron acceptors instead of native cytochrome *c*. Native cytochrome *c*, the most widespread detector of O_2^-, was strikingly reduced by direct reduction rather than via O_2^-, so that its use in cell-free combination experiments became unable to show the oxidase activity (Fig. 1A). This direct cytochrome *c* reduction stemmed from the cytosol but not the membranes of GT-treated cells (Fig. 1B). The use of acetylated cytochrome *c* and INT, however, efficiently obviated the side reaction (Fig. 1C). Using these electron acceptors for the cell-free combination experiments, we were finally able to show that the membrane com-

ponent (i.e., flavocytochrome b_{558}), but not cytosolic ones, was directly affected in the GT-treated neutrophils (Table 1).

Next, we examined the direct effect of GT on the cell-free activation of NADPH oxidase by using membranes from untreated cells and recombinant cytosolic components. As expected from the results in Table 1, the membranes treated in vitro with GT also lost 82.7% of the ability to reconstitute O_2^- generation (Table 2). Furthermore, it is noteworthy that the simultaneous presence of GT with native cytochrome *c* in the semirecombinant assay did not cause the above direct reduction observed with the cytosol (Fig. 2A; see the baseline in the presence of GT).

The toxicity of GT to the NADPH oxidase in the semirecombinant assay efficiently occurred during the activation step, but not after the enzyme has been activated (Fig. 3). This fact suggests that the site(s) affected by GT is likely to become inaccessible after the oxidase activation. Furthermore, when a similar amount of flavocytochrome b_{558} was used in the cell-free assays, the IC_{50}s of GT for prior addition were the same (3.3 μM) regardless of the source of cytosolic components, whether the recombinants (assayed with cytochrome *c*, Fig. 2B) or native cytosol (assayed with acetylated cytochrome *c* [data not shown]). The equal IC_{50}s should reflect that the inhibition of the NADPH oxidase with GT occurs based on the deterioration of the membrane component flavocytochrome b_{558} but not of cytosolic ones.

The assembly of flavocytochrome b_{558} with cytosolic components is crucial for the activation of the NADPH oxidase. As mentioned above, GT impeded the membrane translocation of cytosolic *phox* components but not Rac2 in intact cells (57). Thus, it was examined here whether GT also affects the in vitro membrane translocation of cytosolic components after stimulation in the cell-free assay. The membrane translocation of $p67^{phox}$, $p47^{phox}$ (Fig. 5A), and Rac2 (Fig. 5B) occurred normally and revealed that GT is innocuous to the association of flavocytochrome b_{558} with the cytosolic components.

The present cell-free assay, in which the intramolecular binding within $p47^{phox}$ is unmasked upon the stimulation with MA or SDS, proved that GT directly compromises the flavocytochrome b_{558} function for electron flow but not the assembly of the oxidase components. However, we cannot exclude the possibility of GT changing the "quality" of the interactions between flavocytochrome b_{558} and the cytosolic components; in a way, they become assembled but do not acquire the "right" enzyme conformation for catalytic competence.

It is known that GT reacts with cysteine residues accessible in proteins through forming an intermediary mixed disulfide structure; furthermore, if an additional cysteine is adjacent, GT preferentially undergoes reduction to its dithiol form, oxidizing the target protein that is left with a disulfide bond (26). Here, it can be speculated that cysteine residues of flavocytochrome b_{558} were modified by GT. The primary sequence of the $gp91^{phox}$ subunit of flavocytochrome b_{558} shows 12 single cysteines (residues 59, 64, 72, 126, 185, 244, 257, 282, 329, 428, 445, and 537), two neighboring cysteines (residues 369 and 371), and one vicinal pair (Cys85-86). The vicinal Cys85-86 adjoins the reported $p47^{phox}$-binding motif in $gp91^{phox}$ (^{87}STRVRRQL) able to inhibit the cell-free activation of the NADPH oxidase if added as a synthetic peptide (11). Prediction from the primary sequence of $gp91^{phox}$ also maps the Cys85-86 to a loop facing the cytosol (for a review, see reference 59), which means that they could be easily attacked by membrane permeable GT. These cysteines are also quite close to His101, which coordinates a heme, together with His209 (5, 20). This heme is positioned very near the cytoplasmic face of the membrane, in the neighborhood of the FAD-binding site of $gp91^{phox}$ (59). Binding of GT to the vicinal Cys85-86 could have affected critical parameters in the heme-surroundings needed for electron flow but not to the point of drastically perturbing the heme, as demonstrated by the unaltered heme spectrum of GT-treated flavocytochrome b_{558} (Fig. 6).

Another pair of cysteines that deserve attention are those at positions 369 and 371 in the cytoplasmic tail of $gp91^{phox}$. These cysteines, as well as the aforementioned Cys85-86, were previously reported to be candidate sites targeted by PAO (16). PAO forms a ring complex specifically with vicinal or neighboring thiols (52) and, like GT, only inhibits if used before NADPH oxidase activation (16, 33, 37, 40). Thus, the binding of GT to the Cys369 and Cys371, which are located between the FAD- and NADPH-binding sites of $gp91^{phox}$, may also affect the electron transfer. Finally, the possibility that targeting of any single cysteines by GT may contribute to the inhibition of the electron transfer also cannot be excluded. The other subunit of flavocytochrome b_{558}, $p22^{phox}$, has only two cysteines considerably separated each other (residues 50 and 113), thus making damage through formation of disulfide bond between them less probable. Indeed, GT did not inhibit the interaction between $p22^{phox}$ and $p47^{phox}$ (Fig. 5A), which suggests little effect of GT on $p22^{phox}$.

The high incidence of aspergillosis in chronic granulomatous disease patients suggests that ROS produced by neutrophils are a crucial weapon against *Aspergillus* spp. (9, 27, 51). Thus, the most effective way for *Aspergillus* spp. to show virulence is to attack the phagocyte NADPH oxidase with GT. In the present study, we have demonstrated by using the cell-free activation assay that GT directly affects the NADPH oxidase component, flavocytochrome b_{558}. The inhibition by GT most likely consists of preventing flavocytochrome b_{558} from functioning as the redox center. Since the direct effect of GT on flavocytochrome b_{558} also occurred in intact neutrophils (Table 1), it is likely that, in the course of infection, GT-producing pathogenic *Aspergillus* escape the host defense-committed neutrophil NADPH oxidase in at least two ways: by inhibiting the protein kinase C βII-related responses necessary for oxidase assembly (57) and by inhibiting the flavocytochrome b_{558}-based redox reactions described in the present study. This double targeting of the ROS-based defense by GT would make it easier for the toxin-producing strains to accomplish rapid mycelial growth, thus increasing the risk of invasive aspergillosis even in an immunocompetent host.

ACKNOWLEDGMENTS

This study was partly supported by grants from the Japan Society for the Promotion of Science and from the Human Science Research Foundation of Japan.

We are grateful to J. D. Lambeth for providing cDNA for *r*$p47^{phox}$ and *r*$p67^{phox}$.

REFERENCES

1. **Ago, T., H. Nunoi, T. Ito, and H. Sumimoto.** 1999. Mechanism for phosphorylation-induced activation of the NADPH oxidase protein $p47^{phox}$: triplet

replacement of serines 303, 304, and 328 with aspartates disrupts the SH3 domain-mediated intramolecular interaction in p47^{phox}, thereby activating the oxidase. J. Biol. Chem. **274:**33644–33653.
2. **Akard, L. P., D. English, and T. G. Gabig.** 1988. Rapid deactivation of NADPH oxidase in neutrophils: continuous replacement by newly activated enzyme sustains the respiratory burst. Blood **72:**322–327.
3. **Babior, B. M.** 1999. NADPH oxidase: an update. Blood **93:**1464–1476.
4. **Bauer, J., M. Gareis, A. Bott, and B. Gedek.** 1989. Isolation of a mycotoxin (gliotoxin) from a bovine udder infected with *Aspergillus fumigatus*. J. Med. Vet. Mycol. **27:**45–50.
5. **Biberstine-Kinkade, K. J., F. R. DeLeo, R. I. Epstein, B. A. LeRoy, W. M. Nauseef, and M. C. Dinauer.** 2001. Heme-ligating histidines in flavocytochrome b_{558}: identification of specific histidines in gp91^{phox}. J. Biol. Chem. **276:**31105–31112.
6. **Bromberg, Y., and E. Pick.** 1985. Activation of NADPH-dependent superoxide production in a cell-free system by sodium dodecyl sulfate. J. Biol. Chem. **260:**13539–13545.
7. **Cross, A. R., F. R. Higson, O. T. G. Jones, A. M. Harper, and A. W. Segal.** 1982. The enzymic reduction and kinetics of oxidation of cytochrome b_{245} of neutrophils. Biochem. J. **204:**479–485.
8. **Cross, A. R., J. F. Parkinson, and O. T. G. Jones.** 1984. The superoxide-generating oxidase of leukocytes. NADPH-dependent reduction of flavin and cytochrome *b* in solubilized preparations. Biochem. J. **223:**337–344.
9. **Curnutte, J. T.** 1992. Disorders of granulocyte function and granulopoiesis, p. 904–937. *In* N. Oski (ed.), Hematology of infancy and childhood, 4th ed. The W. B. Saunders Co., Philadelphia, Pa.
10. **Dekker, L. V., M. Leitges, G. Altschuler, N. Mistry, A. McDermott, J. Roes, and A. W. Segal.** 2000. Protein kinase C-β contributes to NADPH oxidase activation in neutrophils. Biochem. J. **347:**285–289.
11. **DeLeo, F. R., L. Yu, J. B. Burritt, L. R. Loetterle, C. W. Bond, A. J. Jesaitis, and M. T. Quinn.** 1995. Mapping sites of interaction of p47-*phox* and flavocytochrome *b* with random-sequence peptide phage display libraries. Proc. Natl. Acad. Sci. USA **92:**7110–7114.
12. **Diebold, B. A., and G. M. Bokoch.** 2001. Molecular basis for Rac2 regulation of phagocyte NADPH oxidase. Nat. Immunol. **2:**211–215.
13. **Diekmann, D., A. Abo, C. Johnston, A. W. Segal, and A. Hall.** 1994. Interaction of Rac with p67^{phox} and regulation of phagocytic NADPH oxidase activity. Science **265:**531–533.
14. **Dinauer, M. C.** 2003. Regulation of neutrophil function by Rac GTPases. Curr. Opin. Hematol. **10:**8–15.
15. **Dorseuil, O., M. T. Quinn, and G. M. Bokoch.** 1995. Dissociation of Rac translocation from p47^{phox}/p67^{phox} movements in human neutrophils by tyrosine kinase inhibitors. J. Leukoc. Biol. **58:**108–113.
16. **Doussière, J., A. Poinas, C. Blais, and P. V. Vignais.** 1998. Phenylarsine oxide as an inhibitor of the activation of the neutrophil NADPH oxidase. Identification of the **β** subunit of the flavocytochrome *b* component of the NADPH oxidase as a target site for phenylarsine oxide by photoaffinity labeling and photoinactivation. Eur. J. Biochem. **251:**649–658.
17. **Dusi, S., M. Donini, and F. Rossi.** 1996. Mechanisms of NADPH oxidase activation: translocation of p40^{phox}, Rac1 and Rac2 from the cytosol to the membranes in human neutrophils lacking p47^{phox} or p67^{phox}. Biochem. J. **314:**409–412.
18. **Eichner, R. D., P. Waring, A. M. Geue, A. W. Braithwaite, and A. Müllbacher.** 1988. Gliotoxin causes oxidative damage to plasmid and cellular DNA. J. Biol. Chem. **263:**3772–3777.
19. **El Benna, J., L. P. Faust, and B. Babior.** 1994. The phosphorylation of the respiratory burst oxidase component p47^{phox} during neutrophil activation. Phosphorylation of sites recognized by protein kinase *c* and proline-directed kinases. J. Biol. Chem. **269:**23431–23436.
20. **Finegold, A. A., K. P. Shatwell, A. W. Segal, R. D. Klausner, and A. Dancis.** 1996. Intramembrane *bis*-heme motif for transmembrane electron transport conserved in a yeast iron reductase and the human NADPH oxidase. J. Biol. Chem. **271:**31021–31024.
21. **Fuchs, A., M. C. Dagher, J. Fauré, and P. V. Vignais.** 1996. Topological organization of the cytosolic activating complex of the superoxide-generating NADPH-oxidase: pinpointing the sites of interaction between p47^{phox}, p67^{phox}, and p40^{phox} using the two-hybrid system. Biochim. Biophys. Acta **1312:**39–47.
22. **Gabig, T. G., and B. A. Lefker.** 1985. Activation of the human neutrophil NADPH oxidase results in coupling of electron carrier function between ubiquinone-10 and cytochrome b_{559}. J. Biol. Chem. **260:**3991–3995.
23. **Groemping, Y., K. Lapouge, S. J. Smerdon, and K. Rittinger.** 2003. Molecular basis of phosphorylation-induced activation of the NADPH oxidase. Cell **113:**343–355.
24. **Heyworth, P. G., B. P. Bohl, G. M. Bokoch, and J. T. Curnutte.** 1994. Rac translocates independently of the neutrophil NADPH oxidase components p47^{phox} and p67^{phox}: evidence for its interaction with flavocytochrome b_{558}. J. Biol. Chem. **269:**30749–30752.
25. **Huang, J., and M. E. Kleinberg.** 1999. Activation of the phagocyte NADPH oxidase protein p47^{phox}. Phosphorylation controls SH3 domain-dependent binding to p22^{phox}. J. Biol. Chem. **274:**19731–19737.
26. **Hurne, A. M., C. L. L. Chai, and P. Waring.** 2000. Inactivation of rabbit muscle creatine kinase by reversible formation of an internal disulfide bond induced by the fungal toxin gliotoxin. J. Biol. Chem. **275:**25202–25206.
27. **Johnston, R. B., Jr.** 2001. Clinical aspects of chronic granulomatous disease. Curr. Opin. Hematol. **8:**17–22.
28. **Knaus, U. G., P. G. Heyworth, B. T. Kinsella, J. T. Curnutte, and G. M. Bokoch.** 1992. Purification and characterization of Rac 2: a cytosolic GTP-binding protein that regulates the human neutrophil NADPH oxidase. J. Biol. Chem. **267:**23575–23582.
29. **Kobayashi, T., S. Tsunawaki, and H. Seguchi.** 2001. Evaluation of the process for superoxide production by NADPH oxidase in human neutrophils: evidence for cytoplasmic origin of superoxide. Redox Rep. **6:**27–36.
30. **Koga, H., H. Terasawa, H. Nunoi, K. Takeshige, F. Inagaki, and H. Sumimoto.** 1999. Tetratricopeptide repeat (TPR) motifs of p67^{phox} participate in interaction with the small GTPase Rac and activation of the phagocyte NADPH oxidase. J. Biol. Chem. **274:**25051–25060.
31. **Korchak, H. M., and L. E. Kilpatrick.** 2001. Roles for βII-protein kinase C and RACK1 in positive and negative signaling for superoxide anion generation in differentiated HL60 cells. J. Biol. Chem. **276:**8910–8917.
32. **Kreck, M. L., D. J. Uhlinger, S. R. Tyagi, K. L. Inge, and J. D. Lambeth.** 1994. Participation of the small molecular weight GTP-binding protein Rac1 in cell-free activation and assembly of the respiratory burst oxidase: inhibition by a carboxyl-terminal Rac peptide. J. Biol. Chem. **269:**4161–4168.
33. **Kutsumi, H., K. Kawai, R. B. Johnston, Jr., and K. Rokutan.** 1995. Evidence for participation of vicinal dithiols in the activation sequence of the respiratory burst of human neutrophils. Blood **85:**2559–2569.
34. **Kwong, C. H., H. L. Malech, D. Rotrosen, and T. L. Leto.** 1993. Regulation of the human neutrophil NADPH oxidase by rho-related G-proteins. Biochemistry **32:**5711–5717.
35. **Lambeth, J. D., G. Cheng, R. S. Arnold, and W. A. Edens.** 2000. Novel homologues of gp91^{phox}. Trends Biochem. Sci. **25:**459–461.
36. **Lambeth, J. D.** 2004. Nox enzymes and the biology of reactive oxygen. Nat. Rev. Immunol. **4:**181–189.
37. **Le Cabec, V., and I. Maridonneau-Parini.** 1995. Complete and reversible inhibition of NADPH oxidase in human neutrophils by phenylarsine oxide at a step distal to membrane translocation of the enzyme subunits. J. Biol. Chem. **270:**2067–2073.
38. **Leto, T. L., M. C. Garrett, H. Fujii, and H. Nunoi.** 1991. Characterization of neutrophil NADPH oxidase factors p47-*phox* and p67-*phox* from recombinant baculoviruses. J. Biol. Chem. **266:**19812–19818.
39. **Leto, T. L., A. G. Adams, and I. de Mendez.** 1994. Assembly of the phagocyte NADPH oxidase: binding of Src homology 3 domains to proline-rich targets. Proc. Natl. Acad. Sci. USA **91:**10650–10654.
40. **Li, J., and R. J. Guillory.** 1997. Purified leukocyte cytochrome b_{558} incorporated into liposomes catalyzes a cytosolic factor dependent diaphorase activity. Biochemistry **36:**5529–5537.
41. **Light, D. R., C. Walsh, A. M. O'Callaghan, E. J. Goetzl, and A. I. Tauber.** 1981. Characteristics of the cofactor requirements for the superoxide-generating NADPH oxidase of human polymorphonuclear leukocytes. Biochemistry **20:**1468–1476.
42. **Miki, T., L. S. Yoshida, and K. Kakinuma.** 1992. Reconstitution of superoxide-forming NADPH oxidase activity with cytochrome b_{558} purified from porcine neutrophils: requirement of a membrane-bound flavin enzyme for reconstitution of activity. J. Biol. Chem. **267:**18695–18701.
43. **Minakami, S., K. Titani, and H. Ishikura.** 1958. The structure of cytochrome c. II. Properties of acetylated cytochrome c. J. Biochem. **45:**341–348.
44. **Mizunari, H., K. Kakinuma, K. Suzuki, H. Namiki, T. Kuratsuji, and S. Tsunawaki.** 1993. Nucleoside-triphosphate binding of the two cytosolic components of the respiratory burst oxidase system: evidence for its inhibition by the 2′,3′-dialdehyde derivative of NADPH and desensitization in their translocated states. Biochim. Biophys. Acta **1220:**21–30.
45. **Munday, R.** 1982. Studies on the mechanism of toxicity of the mycotoxin, sporidesmin. I. Generation of superoxide radical by sporidesmin. Chem. Biol. Interact. **41:**361–374.
46. **Nisimoto, Y., J. L. R. Freeman, S. A. Motalebi, M. Hirshberg, and J. D. Lambeth.** 1997. Rac binding to p67^{phox}: structural basis for interactions of the Rac1 effector region and insert region with components of the respiratory burst oxidase. J. Biol. Chem. **272:**18834–18841.
47. **Park, J.-W., H.-S. Park, and S. M. Lee.** 1998. Possible target components for the inhibitory effect of *N*-ethylmaleimide on the activation of neutrophil NADPH oxidase. Biochem. Mol. Biol. Int. **45:**699–707.
48. **Pick, E., Y. Bromberg, S. Shpungin, and R. Gadba.** 1987. Activation of the superoxide forming NADPH oxidase in a cell-free system by sodium dodecyl sulfate: characterization of the membrane-associated component. J. Biol. Chem. **262:**16476–16483.
49. **Poinas, A., J. Gaillard, P. Vignais, and J. Doussière.** 2002. Exploration of the diaphorase activity of neutrophil NADPH oxidase: critical assessment of the interaction of iodonitrotetrazolium with the oxidase redox components. Eur. J. Biochem. **269:**1243–1252.
50. **Shah, D. T., S. Jackman, J. Engle, and B. Larsen.** 1998. Effect of gliotoxin on human polymorphonuclear neutrophils. Infect. Dis. Obstet. Gynecol. **6:**168–175.
51. **Segal, B. H., E. S. DeCarlo, K. J. Kwon-Chung, H. L. Malech, J. I. Gallin,**

and S. M. Holland. 1998. *Aspergillus nidulans* infection in chronic granulomatous disease. Medicine **77:**345–354.
52. **Stockton, L. A., and R. H. S. Thompson.** 1946. British Anti-Lewisite 1: arsenic derivatives of thiol proteins. Biochem. J. **40:**529–535.
53. **Sumimoto, H., Y. Kage, H. Nunoi, H. Sasaki, T. Nose, Y. Fukumaki, M. Ohno, S. Minakami, and K. Takeshige.** 1994. Role of *Src* homology 3 domains in assembly and activation of the phagocyte NADPH oxidase. Proc. Natl. Acad. Sci. USA **91:**5345–5349.
54. **Tsunawaki, S., and C. F. Nathan.** 1984. Enzymatic basis of macrophage activation: kinetic analysis of superoxide production in lysates of resident and activated mouse peritoneal macrophages and granulocytes. J. Biol. Chem. **259:**4305–4312.
55. **Tsunawaki, S., H. Mizunari, H. Namiki, and T. Kuratsuji.** 1994. NADPH-binding component of the respiratory burst oxidase system: studies using neutrophil membranes from patients with chronic granulomatous disease lacking the β-subunit of cytochrome b_{558}. J. Exp. Med. **179:**291–297.
56. **Tsunawaki, S., S. Kagara, K. Yoshikawa, L. S. Yoshida, T. Kuratsuji, and H. Namiki.** 1996. Involvement of $p40^{phox}$ in activation of phagocyte NADPH oxidase through association of its carboxyl-terminal, but not its amino-terminal, with $p67^{phox}$. J. Exp. Med. **184:**893–902.
57. **Tsunawaki, S., L. S. Yoshida, S. Nishida, T. Kobayashi, and T. Shimoyama.** 2004. Fungal metabolite gliotoxin inhibits assembly of the human respiratory burst NADPH oxidase. Infect. Immun. **72:**3373–3382.
58. **Uhlinger, D. J., K. L. Inge, M. L. Kreck, S. R. Tyagi, N. Neckelmann, and J. D. Lambeth.** 1992. Reconstitution and characterization of the human neutrophil respiratory burst oxidase using recombinant p47-*phox*, p67-*phox* and plasma membrane. Biochem. Biophys. Res. Commun. **186:**509–516.
59. **Vignais, P. V.** 2002. The superoxide-generating NADPH oxidase: structural aspects and activation mechanism. Cell. Mol. Life Sci. **59:**1428–1459.
60. **Waring, P., R. D. Eichner, and A. Müllbacher.** 1988. The chemistry and biology of the immunomodulating agent gliotoxin and related epipolythiodioxopiperazines. Med. Res. Rev. **8:**499–524.
61. **Yoshida, L. S., F. Saruta, K. Yoshikawa, O. Tatsuzawa, and S. Tsunawaki.** 1998. Mutation at histidine 338 of $gp91^{phox}$ depletes FAD and affects expression of cytochrome b_{558} of the human NADPH oxidase. J. Biol. Chem. **273:**27879–27886.
62. **Yoshida, L. S., S. Abe, and S. Tsunawaki.** 2000. Fungal gliotoxin targets the onset of superoxide-generating NADPH oxidase of human neutrophils. Biochem. Biophys. Res. Commun. **268:**716–723.

Editor: T. R. Kozel